International Journal of Biomedicine 15(4) (2025) 746-751
http://dx.doi.org/10.21103/Article15(4)_OA17

ORIGINAL ARTICLE
Experimental Biology

INTERNATIONAL JOURNAL OF BIOMEDICINE

Curcumin Analogue EF-24 Induces Ferroptosis in Human Multiple Myeloma Cells MM.1S

Liu-Qing Cui, Meng-Yi Yang, Jia-Jun Zhao, Shi-Wei Ma, Guang-Zhou Zhou*

College of Bioengineering, Henan University of Technology, Zhengzhou 450001, China

Abstract

Myeloma is a type of malignant tumor that originates from plasma cells. The curcumin analog EF-24 has demonstrated promising antitumor activity. However, its role in myeloma cell proliferation was unclear. In this study, we found that EF-24 could inhibit the proliferation of multiple myeloma cells (MM.1S) by morphological observation and CCK-8 assay. RNA-sequencing analysis indicated that several genes associated with ferroptosis exhibited differential transcription, which was confirmed by RT-qPCR. Therefore, following detection of ferroptosis-related proteins (GPX4 and SLC7A11) and upregulation in the destruction of mitochondrial cristae and other ferroptosis factors, including MDA, GSH, ROS, and Fe^{2+} concentrations, were conducted in EF-24-treated MM.1S cells, which concluded that EF-24 could induce ferroptosis in myeloma cells. Conversely, the addition of the ferroptosis inhibitor (ferrostatin-1) could reverse the above changes activated by EF-24. Moreover, NOD/SCID mice grafted with MM.1S cells were constructed, and intravenous injection of EF-24 effectively decreased tumor growth and protected normal tissues, as observed by Hematoxylin-Eosin staining. In summary, our results confirm the EF-24-induced ferroptosis in myeloma cells and exhibited a protective role in model mice grown from implanted MM.1S cells in vivo.(**International Journal of Biomedicine. 2025;15(4):746-751.**)

Keywords: Curcumin analogue • ferroptosis • multiple myeloma

For citation: Cui L-Q, Yang M-Y, Zhao J-J, Ma S-W, Zhou G-Z. Curcumin Analogue EF-24 Induces Ferroptosis in Human Multiple Myeloma Cells MM.1S. International Journal of Biomedicine. 2025;15(4):746-751. doi:10.21103/Article15(4)_OA17

Introduction

Multiple myeloma (MM) is a clonal plasma cell malignancy originating from the bone marrow that accounts for approximately 13% of all hematologic cancers and is associated with a range of symptoms, including anemia, bone damage, hypercalcemia, and renal impairment.[1,2] The treatment of MM has changed dramatically in recent years, with a series of advances in therapeutic approaches that have led to improved survival rates; however, the majority of patients eventually relapse.[3] One of the major advances in the treatment of MM in the last decade has been the introduction of the novel drugs thalidomide, bortezomib, and lenalidomide.[4] But obviously, it is not enough, and many more molecules or drugs against multiple myeloma need to be explored.

Curcumin (Cur) is a bioactive polyphenolic compound found in turmeric, which has a variety of pharmacological activities, including anti-inflammatory, antiaging, antidiabetic, and antitumor functions, and so on.[5,6] Although a large number of clinical trials have confirmed curcumin's safety, its low water solubility, rapid metabolism, and poor bioavailability have not yet led to approval as a clinically applicable drug, limiting its application. As a result, beneficial curcumin derivatives or analogues are now being developed to replace curcumin.[7] Among them, curcumin analog EF-24 shows potent antitumor activity and induces autophagy or apoptosis in various tumor cells.[8-10] However, the effect of EF-24 on myeloma cell proliferation is unknown.

Ferroptosis is an oxidative, iron-dependent form of regulated cell death (RCD) that differs from other types in its morphology, biochemistry, and core regulators, as first proposed by Scott Dixon in 2012.[11,12] Ferroptosis can be induced by inhibiting the cystine/glutamate transporter protein (SLC7A11/xCT) and the enzyme glutathione peroxidase 4 (GPX4), which are critical for preventing ferroptosis.[13] Studies have shown that ferroptosis is an adaptive response with tumor suppressive function.[14] The discovery of ferroptosis as a new mode of cell death has opened a new way to think about and treat many diseases.[15] In this study, the curcumin analogue EF-24 was first used to treat human multiple myeloma cells (MM.1S), and the current study demonstrated that EF-24 could inhibit cell proliferation and induce ferroptosis. Furthermore, the in vivo

antitumor effect of EF-24 was investigated in NOD/SCID mice grafted with MM.1S cells.

The present study provided additional information and laid a solid foundation for future research on the antitumor properties of curcuminoids.

Materials and Methods

Cell Culture and Chemicals

The human multiple myeloma cell line MM.1S was purchased from Sebachem (Shanghai Biotechnology Co. Ltd.) and cultured in RPMI-1640 medium containing 10% FBS at 37°C with 5% CO_2.

Cur analogue EF-24 (Sigma-Aldrich, Shanghai, China) was dissolved in dimethyl sulfoxide (DMSO) to prepare a 40 mM master stock solution, which was stored at -20°C before use. Ferrostatin-1 (abbreviated Fer-1, HY-100579), Z-VAD-FMK (HY-16658B), and wortmannin (HY-12420) were purchased from MedChemExpress (MCE, Shanghai, China). Anti-GPX4, SLC7A11, and α-tubulin primary antibodies were bought from ProteinTech (Wuhan, China). The IRDye® 800CW Goat anti-mouse IgG(H+L) and IRDye® 800CW Goat anti-rabbit IgG(H+L) secondary antibodies were provided by Li-Cor Biotechnology (Lincoln, NE, USA).

Cell Viability Assay

MM.1S cells were inoculated into 6-well plates (6×10^5/well) and incubated overnight after treating the cells with different concentrations of EF-24 (0, 200, 400, 600, 800, and 1000 nM) for different times. Morphological changes in treated cells were observed with an inverted microscope and photographed.

For cell viability analysis, MM.1S cells were inoculated into 96-well plates (1×10^4/well) overnight and treated with DMSO and a range of concentrations of EF-24 (0-1000 nM) for different times, respectively. Then, 10 μL of CCK-8 (Uelandy, Suzhou, China) was added to each well and incubated for another 4 h at 37 °C. Finally, cell absorbances were measured with a microplate spectrophotometer at 450 nm.

cDNA Extraction and RNA-Sequencing

MM.1S cells were treated with EF-24 (600 nM) for 24 h, then total RNA was extracted using TRIzol kit (Thermo Fisher, CA, USA). Transcriptome data were obtained using Illumina NovaseqTM 6000 (LC Bio Technology CO., Ltd., Hangzhou, China). GO function analysis, pathway function analysis, cluster analysis, and other in-depth mining analyses were performed on the selected differentially expressed genes. Quantitative analysis of three randomly selected cell death signal-related genes (*p62/SQSTM1, FTL*, and *GJA1*) was conducted using quantitative real-time PCR (qRT-PCR).

qRT-PCR

MM.1S cells were inoculated into 6-well plates and cultured overnight, and then treated with EF-24 at different concentrations for 24 h. The total RNA samples were extracted from the treated cells using a conventional protocol. The RNA samples were reverse transcribed into cDNA. RT-qPCR was performed using a SYBR Green real-time fluorescence quantitative PCR system. The following primer sequences were used for the PCR procedures:

p62/SQSTM1-F: TACGACTTGTGTAGCGTCTGC, *p62/SQSTM1*-R: GTGTCCGTGTTTCACCTTCC

FTL-F: CACGGACCCCCATCTCTGTG, *FTL*-R: TAGTCGTGCTTGAGAGTGAGC

GJA1-F: CCAGCACCGTTTTTGTGGTT, *GJA1*-R: GGTCGAAATAGAAGCCCAGAGA.

GAPDH (F: AATGACCCCTTCATTGAC, R: TCCACGACGTACTCAGCGC) was used as an internal control gene for mRNA quantification. The relative mRNA values for each group were calculated using the $2^{-\Delta\Delta}$Ct method.

Western Blot

The treated MM.1S cells were lysed in lysis buffer containing 2% SDS, 25 mM Tris-HCl (pH 6.8), 2 mM PMSF, 6% glycerol, 0.02% bromophenol blue, 1% β-mercaptoethanol, and protease inhibitors. Proteins were separated by SDS-PAGE, and the target proteins in the gel were transferred to a nitrocellulose membrane (NC), which was then incubated with a primary antibody at 4°C overnight. After washing with TBST, the membranes were incubated with the appropriate secondary antibody for 1 h at room temperature. Immunoblots were processed using an Odyssey CLX infrared imaging system (LI-COR Biosciences, Cambridge, UK), and the fluorescence intensity of the blot was analyzed using the Odyssey application.

MDA and GSH Assay

After MM.1S cells came to approximately 80% confluence in 6-well plates, the cells were exposed to EF-24 (2.5-20 μM) with Fer-1 (2 μM), or Z-VAD-FMK (5 μM), or wortmannin (5 μM) for 24 h, respectively. Total malondialdehyde in treated cells was determined using a malondialdehyde assay kit (Nanjing Jiancheng, China) and normalized to protein concentration according to the manufacturer's instructions. Similarly, for the detection of GSH in treated cells, the total amount of glutathione was determined using a glutathione assay kit (Beyotime Biotechnology, Shanghai, China) and normalized to protein concentration according to the manufacturer's instructions.

Transmission Electron Microscopy (TEM)

After treatment with EF-24 (600 nM) for 24 h, the cells were fixed with a 2% paraformaldehyde-2.5% glutaraldehyde fixation mixture. Next, the cells were dehydrated continuously with graded concentrations (30%, 50%, 70%, 80%, 90%, and 95%) of ethanol solution for 15 min. Anhydrous ethanol and acetone were then used to treat the cells for 20 min, respectively. After embedding, the cell samples were sectioned with a UC7 Ultrathin Section Ultrathin Slicer. Finally, the cells were stained with uranyl acetate and alkaline lead citrate, respectively. The samples were observed and photographed using a transmission electron microscope (JEOL-JEM-1200EX, Japan).

ROS and Fe^{2+} Fluorescence Assay

MM.1S cells were inoculated into 6-well plates (1×10^5/well) and cultured overnight. The cells were treated with EF-24

or EF-24 (5 μM) + Fer-1 (1 μM) for 24 h, respectively (Rousp-treated cells for 30 min were used as a positive control). After aspiration of the waste liquid, DCFH-DA probe (10 mM, diluted in serum-free culture medium at 1:1000) was added to the wells for 15 min at 37°C. The cells were then thoroughly washed with serum-free cell culture solution and resuspended in PBS. ROS levels in different samples were measured using flow cytometry (BD FACSCanto™ II, USA).

As for the detection of Fe^{2+} concentrations in cells treated with the above-described methods, the cell supernatant was discarded, and the cells were washed three times with PBS. Finally, FerroOrange working solution (1 μM) was added into the wells, and the cell plates were visualized using a fluorescence microscope (ZEISS AxioObserver 3, Germany).

Hematoxylin-Eosin (HE) Staining

SPF-grade female NOD/SCID mice (Beijing Viton Lever, n=6, 4-6 weeks old, weight 20~25 g) were purchased and fed in a SPF-grade sterile laminar flow animal rearing system. The density of MM.1S was adjusted to 7×10^7 cells/mL, and each mouse was inoculated with 150 μL subcutaneously on the dorsal surface of the left hind limb. The modeled mice were injected with saline and EF-24 (200 μL/per mouse, 20 mg/kg) into the tail vein every 3 days, according to standard procedures. After 7 injections, the treated mice were sacrificed for histochemical analysis. Then, the heart, liver, spleen, lung, kidney, and tumor tissues of the mice were dissected for ultrathin sectioning. The tissue sections were stained with HE and photographed under a microscope.

Statistical Analysis

The significance of differences between groups was tested using t-test. GraphPad Prism 7.0c software was used for statistical analysis. A *P*-value <0.05 was considered statistically significant.

Results

EF-24 Inhibits MM.1S Cell Proliferation

Inverted microscopy revealed that the morphology of the EF-24-treated cells in the experimental group underwent significant changes, including fragmentation, shrinkage, and death, whereas the control group showed normal cell growth (Figure 1A). As the concentration increases, the damage to the treated cells gradually intensifies. In addition, we examined the effect of EF-24 on MM.1S cell proliferation using the CCK-8 assay (Figure 1B). The results showed that higher concentrations and longer treatment times were associated with greater decreases in cell viability, suggesting that EF-24 inhibits MM.1S cell proliferation in a time- and concentration-dependent manner.

EF-24 Induces the Expression of Ferroptosis-related Genes Differently in MM.1S Cells

To explore the potential antitumor mechanism of EF-24 against MM.1S, we first used transcriptomic analysis to identify differentially expressed genes in EF-24-treated MM. 1S cells. Three replicate samples from the EF-24-treated groups or the blank control groups were collected for RNA-seq analysis. The present results showed that 292 genes were upregulated and 539 were downregulated. Heat map and volcano plot analyses showed that among the upregulated genes, *GJA1*, *FTL*, and *p62/SQSTM1* were the most differentially expressed (Figure 2A).

Therefore, qRT-PCR was performed to identify transcriptional changes in the three genes in EF-24-treated MM.1S cells. Current results confirmed that *GJA1*, *FTL*, and *p62/SQSTM1* mRNA levels were elevated compared with the blank control group (Figure 2B), consistent with transcriptome sequencing analysis. Given that genes such as *GJA1* and *FTL* are involved in ferroptosis, we speculated that differential expression of ferroptosis-related genes in MM.1S cells may be associated with EF-24 treatment.

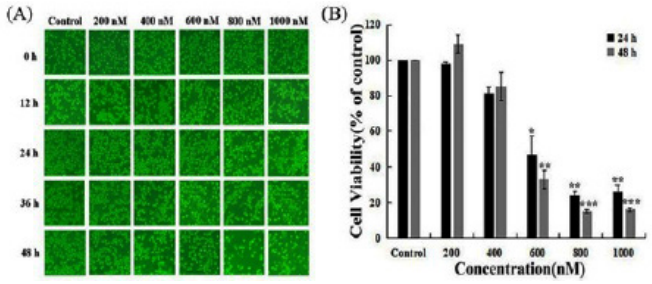

Fig. 1. *Effect of EF-24 on the proliferation of MM.1S cells. (A) Morphological changes of MM.1S cells after treatment with different concentrations of EF-24 for different times (original magnification, ×100). (B) Cell viability analysis of MM.1S cells treated with different concentrations of EF-24 for 24 and 48 h (n=3; *-P<0.05, **-P<0.01, and ***-P<0.001).*

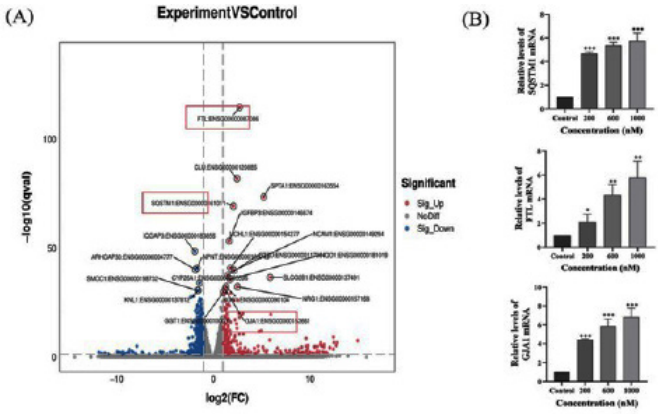

Fig.2. *Transcriptomic analysis of cell-death-related genes in EF-24-treated MM.1S cells. (A) Volcano map analysis of transcriptome sequencing differential gene clustering after EF-24 treatment of MM.1S cells. Several cell death-related genes were outlined in red. (B) RT-qPCR analysis of FTL, GJA1, and p62/SQSTM1 mRNA after 24 h of treatment with different concentrations of EF-24 (n=3; **- P<0.01 and *** - P<0.001).*

EF-24 Induces Ferroptosis in MM.1S Cells

When ferroptosis occurs, several changes occur within the cell, including the accumulation of MDA, ROS, and Fe^{2+}, depletion of GSH, and changes in mitochondrial morphology. Here, we firstly treated MM.1S cells with various concentrations of EF-24 and assessed changes in cellular MDA and GSH levels. Relative to the untreated cells, the experimental group

exhibited increased MDA levels and decreased GSH levels with a concentration-dependent effect (from 200 nM to 1000 nM) (Figure 3A; 3B), respectively. Subsequently, following treatment with EF-24 (600 nM), fluorescence microscopy analysis showed stronger orange-red fluorescence in the experimental group compared to the control (Figure 3C), suggesting elevated Fe^{2+} levels in the experimental group. Moreover, flow cytometry analysis was applied to detect the production of ROS in EF-24-treated MM.1S cells, which showed that the ROS level had an increasing trend in a concentration-dependent manner (from 200 nM to 1000 nM of EF-24) (Figure 3D). Additionally, transmission electron microscopy of MM.1S cells treated with EF-24 (600 nM) showed that mitochondrial volume and cristae decreased or disappeared. At the same time, there were no apparent changes in the control group (Figure 3E). In summary, these results suggested that EF-24 indeed induced ferroptosis in MM.1S cells.

Furthermore, we continued to detect the expression of two key regulatory factors of ferroptosis, GPX4 and SLC7A11, which are considered upstream regulators of ferroptosis. The present study indicated that, after EF-24 treatment, the expressions of GPX4 and SLC7A11 were downregulated overall (Figure 3F), further supporting EF-24-induced ferroptosis.

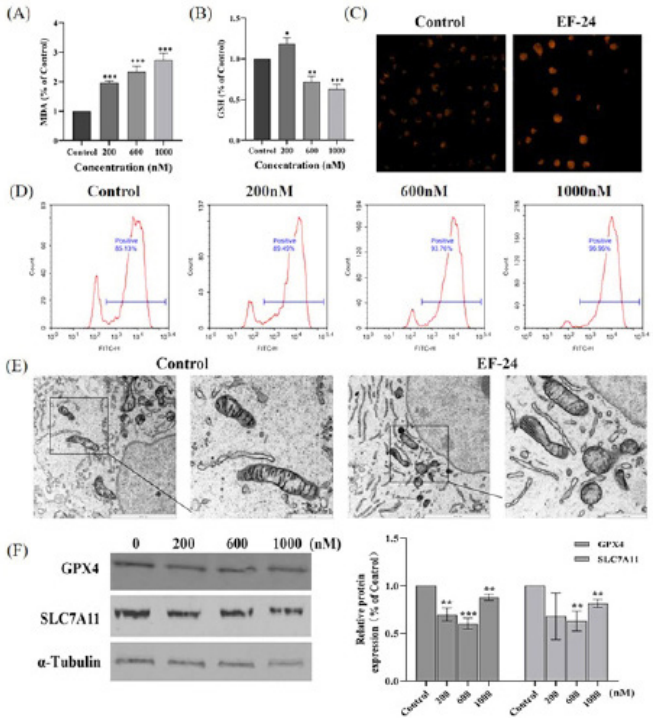

Fig.3. *EF-24 induces ferroptosis in MM.1S cells. (A) and (B) Changes of MDA and GSH content in cells treated with different concentrations of EF-24 for 24 h, respectively. (C) Cells were treated with EF-24 (600 nM) for 24 h. The Fe^{2+} concentrations (yellow color) were observed by fluorescence microscopy. (D) Cells were treated with different concentrations of EF-24 for 24 h, and ROS levels were detected using flow cytometry. (E) Cells were treated with EF-24 (600 nM) for 24 h, and the changes in mitochondria were observed by transmission electron microscopy. (F) Western blot analysis (Left) and statistical analysis (Right) of GPX4 and SLC7A11 after treatment with different concentrations of EF-24 for 24 h. Bars represent densitometric analysis of the ratio of GPX4 or SLC7A11 to GAPDH expression levels. (n=3; *-P<0.05, **-P<0.01, and ***- P<0.001).*

Addition of Inhibitors Suppresses Ferroptosis in MM.1S Cells

To further confirm ferroptosis induced by EF-24 in MM.1S cells, after combination treatment with EF-24 (600 nM) and the ferroptosis inhibitor ferrostatin-1 (2 μM), we found that MDA levels were reduced, while GSH levels were significantly increased compared to the EF-24-alone treatment group. However, the MDA levels in the groups treated with the combination of EF-24 and either the autophagy inhibitor wortmannin (5 μM) or the apoptosis inhibitor Z-VAD-FMK (5 μM) remained essentially unchanged or even slightly increased, while GSH levels remained essentially unchanged or even decreased (Figure 4A; 4B). Additionally, the number of intracellular orange-red fluorescence signals was significantly reduced in the combination treatment group with ferrostatin-1 (Figure 4C), indicating that the addition of ferrostatin-1 led to a significant decrease in cellular Fe^{2+} levels in EF-24-treated MM.1S cells. Moreover, flow cytometry analysis showed that the ROS level in the combination treatment group was significantly lower than in the EF-24-alone treatment group. These results further confirmed that EF-24 induced ferroptosis in MM.1S cells.

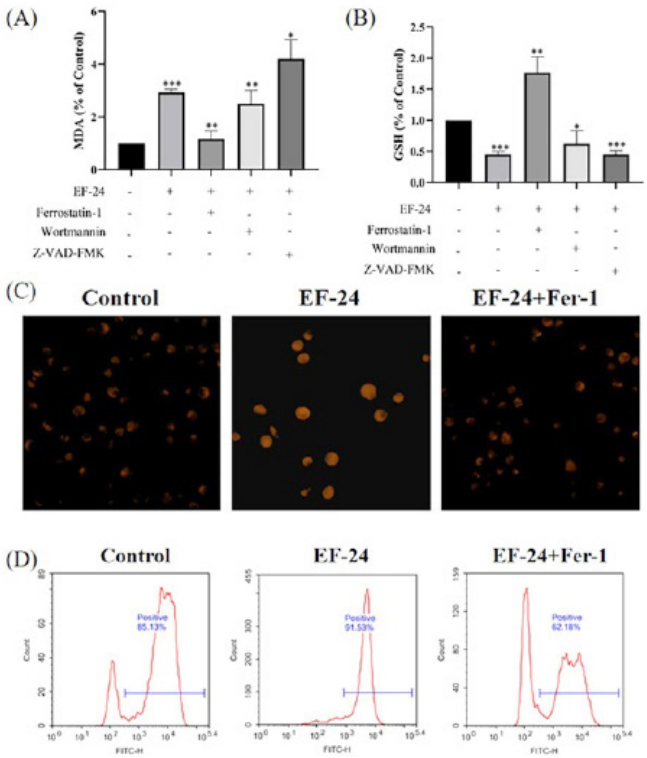

Fig. 4. *Ferrostatin-1 (Fer-1) inhibits EF-24-inducing ferroptosis in MM.1S cells. Expression of MDA (A) and GSH (B) in cells treated with EF-24 (600 nM), and EF-24 (600 nM) in combination with Ferrostatin-1 (2 μM), Z-VAD-FMK (5 μM), or Wortmannin (5 μM) for 24 h, respectively. (C) Fluorescence microscopy for Fe^{2+} content after co-treatment of cells with EF-24 (600 nM) or EF-24 (600 nM) with Fer-1 (2 μM), respectively. (D) ROS expression was detected by flow cytometry after cells were co-treated with EF-24 (600 nM) or EF-24 (600 nM) with Fer-1 (2 μM), respectively (n=3; *-P<0.05, **-P<0.01, and ***-P<0.001).*

EF-24 Can Resist Tumor Progress *in vivo*

To further determine the in vivo antitumor proliferation ability of EF-24, NOD/SCID mouse models grafted with

MM.1S cells were constructed, and EF-24 was administered to treat the mice. After 15 days of treatment, the overall tumor inhibition rate reached 47.25% in EF-24-injected mice, with tumor volumes and sizes significantly reduced compared to control mice. The current study suggested that EF-24 could block tumor progression in vivo.

In addition, tumor tissue from mice and normal organ tissue were collected for HE staining analysis. The results showed that normal heart, liver, spleen, lung, and kidney tissue from mice treated with EF-24 retained a relatively compact structure and had fewer cavities compared to the control groups (Figure 5). Tumor tissue from mice treated with EF-24 was significantly damaged by EF-24 and had more cavities per section (Figure 5). These results clearly demonstrated the ability of EF-24 to suppress tumor cell proliferation in vivo.

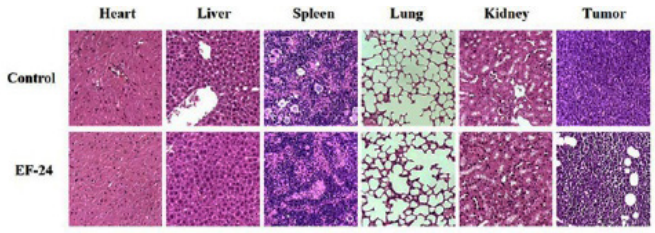

Fig.5. *HE-staining analysis of tissues from NOD/SCID mouse models grafted with MM.1S cells. EF-24 treatment could effectively protect normal organs while damaging tumor tissues in mice.*

Discussion

Although significant progress has been made over the past two decades in the study of the physiopathological mechanisms underlying myeloma,[16] myeloma remains a hitherto incurable plasma cell malignancy. Developing more antimyeloma strategies or drug molecules has become an urgent task.

In our previous study, we confirmed the anti-proliferative and anti-migratory activities of the curcumin analogue EF-24 against breast cancer cells.[17,18] Even recently, we have discovered that EF-24 has antiviral effects on rhabdovirus replication.[19] In fact, compared with curcumin, EF-24 exhibited better bioavailability and antitumor activity. Several studies have demonstrated that EF-24 can inhibit cancer development through various pathways, including inhibition of the NF-κB and p38 pathways and regulation of ROS production.[20,21] However, its role in myeloma remains unexplored. Therefore, this study aimed to investigate the mechanism of EF-24 against myeloma cell proliferation.

The current study confirmed that EF-24 had the ability to inhibit the proliferation of human multiple myeloma cells, MM.1S. Transcriptomic sequencing and subsequent qRT-PCR analysis suggested that ferroptosis-related genes were regulated following EF-24 treatment in MM.1S cells. As a type of cell death caused by lipid peroxidation, ferroptosis plays an important role in tumor suppression and can provide new ideas and methods for cancer treatment.[22] When ferroptosis occurs, a series of physiological and biochemical changes occurs within the cell.[23] Therefore, experiments were performed to verify cell ferroptosis in EF-24-treated MM.1S cells by fluorescence microscopy, transmission electron microscopy, and flow cytometry. By promoting Fe^{2+} and ROS accumulation, increasing MDA levels, suppressing GSH, and reducing mitochondrial cristae, EF-24 triggers ferroptosis in MM.1S cells. GPX4 and SLC7A11, key regulators of ferroptosis, were also assessed by western blot, which showed downregulation of their expression in EF-24-treated MM. 1S cells, further confirming EF-24-Induced ferroptosis in MM.1S cells.

In fact, for multiple myeloma (MM), some potential antitumor molecules or extracts had been developed and characterized in previous reports. Zhong et al.[24] found that fingolimod (FTY720), a novel immunosuppressant, could induce ferroptosis and autophagy via the PP2A/AMPK pathway in myeloma cell lines U266 and RPMI8266, providing a new perspective on the MM treatment. Recently, Li et al.[25] also identified several molecules or compounds that can significantly induce ferroptosis in MM cells, including ethanol extract of Eclipta prostrata, andrographolide,[26] and shikonin.[27] Liang et al.[28] also found that the antimalarial drug artesunate (ART) could inhibit nuclear localization of SREBP2, downregulate IPP and GPX4, and eventually trigger ferroptosis in myeloma cells. All these compounds could be considered as potential drug candidates against myeloma. Our present study on the mediation of ferroptosis in MM.1S by EF-24 may identify a new candidate molecule for antimyeloma therapy.

We should note that although some compounds that sensitize myeloma cells to ferroptosis have been screened and are appealing alternative treatment strategies for multiple myeloma and other malignancies, only a limited number of ferroptosis regulators or factors have been identified.[29] Further research should aim to elucidate the detailed mechanism of interaction between ferroptosis and myeloma-targeting drugs. Our current study certainly opens new possibilities for myeloma treatment and potential clinical applications.

Funding Statement

This research was supported by the Natural Science Foundation of Henan (232300420018) and the High-level talents Fund from Henan University of Technology (2023BS001).

Competing Interests

The authors declare that they have no financial/commercial conflicts of interest concerning this article.

References

1. Kyle RA, Rajkumar SV. Multiple myeloma. Blood. 2008 Mar 15;111(6):2962-72. doi: 10.1182/blood-2007-10-078022.
2. Joshua DE, Bryant C, Dix C, Gibson J, Ho J. Biology and therapy of multiple myeloma. Med J Aust. 2019 May;210(8):375-380. doi: 10.5694/mja2.50129.
3. Pawlyn C, Davies FE. Toward personalized treatment in multiple myeloma based on molecular characteristics.

Blood. 2019 Feb 14;133(7):660-675. doi: 10.1182/blood-2018-09-825331.
4. Moreau P, Attal M, Facon T. Frontline therapy of multiple myeloma. Blood. 2015 May 14;125(20):3076-84. doi: 10.1182/blood-2014-09-568915.
5. Yavarpour-Bali H, Ghasemi-Kasman M, Pirzadeh M. Curcumin-loaded nanoparticles: a novel therapeutic strategy in treatment of central nervous system disorders. Int J Nanomedicine. 2019 Jun 17;14:4449-4460. doi: 10.2147/IJN.S208332.
6. Anand P, Kunnumakkara AB, Newman RA, Aggarwal BB. Bioavailability of curcumin: problems and promises. Mol Pharm. 2007 Nov-Dec;4(6):807-18. doi: 10.1021/mp700113r.
7. Tomeh MA, Hadianamrei R, Zhao X. A Review of Curcumin and Its Derivatives as Anticancer Agents. Int J Mol Sci. 2019 Feb 27;20(5):1033. doi: 10.3390/ijms20051033.
8. Hsiao PC, Chang JH, Lee WJ, Ku CC, Tsai MY, Yang SF, Chien MH. The Curcumin Analogue, EF-24, Triggers p38 MAPK-Mediated Apoptotic Cell Death via Inducing PP2A-Modulated ERK Deactivation in Human Acute Myeloid Leukemia Cells. Cancers (Basel). 2020 Aug 4;12(8):2163. doi: 10.3390/cancers12082163.
9. Skoupa N, Dolezel P, Ruzickova E, Mlejnek P. Apoptosis Induced by the Curcumin Analogue EF-24 Is Neither Mediated by Oxidative Stress-Related Mechanisms nor Affected by Expression of Main Drug Transporters ABCB1 and ABCG2 in Human Leukemia Cells. Int J Mol Sci. 2017 Oct 31;18(11):2289. doi: 10.3390/ijms18112289.
10. Shi YY, Zhou GZ, Li AF, Zhou YH. Review on the cellular anti-proliferation research development of curcumin analogs. Biotechnology. 2017; **27**, 192-197.
11. Li J, Cao F, Yin HL, Huang ZJ, Lin ZT, Mao N, Sun B, Wang G. Ferroptosis: past, present and future. Cell Death Dis. 2020 Feb 3;11(2):88. doi: 10.1038/s41419-020-2298-2.
12. Tang D, Chen X, Kang R, Kroemer G. Ferroptosis: molecular mechanisms and health implications. Cell Res. 2021 Feb;31(2):107-125. doi: 10.1038/s41422-020-00441-1.
13. Lei ZY, Li ZH, Lin DN, Cao J, Chen JF, Meng SB, et al. Med1 inhibits ferroptosis and alleviates liver injury in acute liver failure via Nrf2 activation. Cell Biosci. 2024 Apr 27;14(1):54. doi: 10.1186/s13578-024-01234-4.
14. Guo L, Wang Z, Fu Y, Wu S, Zhu Y, Yuan J, Liu Y. MiR-122-5p regulates erastin-induced ferroptosis via CS in nasopharyngeal carcinoma. Sci Rep. 2024 May 1;14(1):10019. doi: 10.1038/s41598-024-59080-w.
15. Lai L, Tan M, Hu M, Yue X, Tao L, Zhai Y, Li Y. Important molecular mechanisms in ferroptosis. Mol Cell Biochem. 2025 Feb;480(2):639-658. doi: 10.1007/s11010-024-05009-w.
16. Bazou D, Dowling P. Editorial: Multiple Myeloma: Molecular Mechanism and Targeted Therapy. Int J Mol Sci. 2024 Mar 28;25(7):3799. doi: 10.3390/ijms25073799.
17. Li J, Wang SH, Liu YT, Zhang Q, Zhou GZ. Inhibition of autophagic flux by the curcumin analog EF-24 and its antiproliferative effect on MCF-7 cancer cells. J Biochem Mol Toxicol. 2023 Apr;37(4):e23307. doi: 10.1002/jbt.23307.
18. Zhao YY, Li J, Wang HQ, Zheng HB, Ma SW, Zhou GZ. Activation of autophagy promotes the inhibitory effect of curcumin analog EF-24 against MDA-MB-231 cancer cells. J Biochem Mol Toxicol. 2024 Feb;38(2):e23642..
19. Ju PM, Ma SW, Li YY, Zhang SF, Li J, Zhou GZ. Investigation of the antiviral mechanism of curcumin analog EF-24 against *Siniperca cachuatsi* rhabdovirus. Fishes. 2024; 9, 179.
20. Lee CY, Ho YC, Lin CW, Hsin MC, Wang PH, Tang YC, Yang SF, Hsiao YH. EF-24 inhibits TPA-induced cellular migration and MMP-9 expression through the p38 signaling pathway in cervical cancer cells. Environ Toxicol. 2023 Feb;38(2):451-459. doi: 10.1002/tox.23709.
21. Su SC, Hsin CH, Lu YT, Chuang CY, Ho YT, Yeh FL, Yang SF, Lin CW. EF-24, a Curcumin Analog, Inhibits Cancer Cell Invasion in Human Nasopharyngeal Carcinoma through Transcriptional Suppression of Matrix Metalloproteinase-9 Gene Expression. Cancers (Basel). 2023 Mar 1;15(5):1552. doi: 10.3390/cancers15051552.
22. Shao L, Zhu L, Su R, Yang C, Gao X, Xu Y, Wang H, Guo C, Li H. Baicalin enhances the chemotherapy sensitivity of oxaliplatin-resistant gastric cancer cells by activating p53-mediated ferroptosis. Sci Rep. 2024 May 10;14(1):10745. doi: 10.1038/s41598-024-60920-y.
23. Zhang W, Li Q, Zhang Y, Wang Z, Yuan S, Zhang X, Zhao M, Zhuang W, Li B. Multiple myeloma with high expression of SLC7A11 is sensitive to erastin-induced ferroptosis. Apoptosis. 2024 Apr;29(3-4):412-423. doi: 10.1007/s10495-023-01909-2.
24. Zhong Y, Tian F, Ma H, Wang H, Yang W, Liu Z, Liao A. FTY720 induces ferroptosis and autophagy via PP2A/AMPK pathway in multiple myeloma cells. Life Sci. 2020 Nov 1;260:118077. doi: 10.1016/j.lfs.2020.118077.
25. Li W, Yin X, Fu H, Liu J, Weng Z, Mao Q, Zhu L, Fang L, Zhang Z, Ding B, Tong H. Ethanol extract of Eclipta prostrata induces multiple myeloma ferroptosis via Keap1/Nrf2/HO-1 axis. Phytomedicine. 2024 Jun;128:155401. doi: 10.1016/j.phymed.2024.155401.
26. Li W, Fu H, Fang L, Chai H, Ding B, Qian S. Andrographolide induced ferroptosis in multiple myeloma cells by regulating the P38/Nrf2/HO-1 pathway. Arch Biochem Biophys. 2023 Jul 1;742:109622. doi: 10.1016/j.abb.2023.109622.
27. Li W, Fu H, Fang L, Chai H, Gao T, Chen Z, Qian S. Shikonin induces ferroptosis in multiple myeloma *via* GOT1-mediated ferritinophagy. Front Oncol. 2022 Oct 25;12:1025067. doi: 10.3389/fonc.2022.1025067.
28. Liang D, Minikes AM, Jiang X. Ferroptosis at the intersection of lipid metabolism and cellular signaling. Mol Cell. 2022 Jun 16;82(12):2215-2227. doi: 10.1016/j.molcel.2022.03.022.
29. Logie E, Van Puyvelde B, Cuypers B, Schepers A, Berghmans H, Verdonck J, Laukens K, Godderis L, Dhaenens M, Deforce D, Vanden Berghe W. Ferroptosis Induction in Multiple Myeloma Cells Triggers DNA Methylation and Histone Modification Changes Associated with Cellular Senescence. Int J Mol Sci. 2021 Nov 12;22(22):12234. doi: 10.3390/ijms222212234.

***Corresponding author**: Guang-Zhou Zhou, E-mail: gzzhou@163.com*